

Allowable Load Assessment in Metal-Composite Double-Lap Joint

Helio de Assis Pegado¹, Rafael Felipe de Souza Almeida², Rodrigo de Sá Martins³

¹*Dept. of Mechanics, Federal University of Minas Gerais - UFMG
Presidente Antonio Carlos Avenue, 6627, 31270-901, Belo Horizonte/MG, Brazil
helio@demec.ufmg.br*

²*Maintenance Engineering Management, Anglo American Iron Ore Brazil
Chiquito Costa Street, 40, 35860-000, Conceição do Mato Dentro/MG, Brazil
rafael.almeida@angloamerican.com*

³*PPGEM, Federal Technological University of Paraná - UTFPR
Doutor Washington Subtil Chueire Street, 330, 84017-220, Ponta Grossa, PR, Brazil
rodrigo.desa.martins@gmail.com*

Abstract. This work consists of evaluating the tensile and compression static allowable stress of a hybrid (metal-composite) riveted joint. The analyzed joint is composed by two sheets of 2014 – T6 aluminium alloy and a T300/5208 Graphite/Epoxy quasi-isotropic laminate, which were joined by twelve Lockbolt Swaged Collar rivets titanium alloy Ti–6Al–4V annealed. The joint was analyzed through a computational model developed using the Finite Element Method (FEM), with the fasteners modelled through the Multi - Springs technique. This method was widely used to simulate the mechanical behaviour metal-metal and composite-composite parts of the joint. It is validated comparing its results with analytical results of metallic joints available in the literature. Through this model, both the allowable load and its distribution in the fasteners of the joint were determined. Since the evaluated joint is subjected to double shear and, therefore, has no eccentricities, the presence of secondary bending was not observed, the bearing and bypass loads were the most relevant in evaluating the allowable loads of the joint. The load distribution in the joint and its components' safety margin was determined, with the laminate being the limiting component of the allowable load.

Keywords: Double-lap Joint, Multi-Springs, Bearing-pass Diagram

1 Introduction

Riveting is one of the most applied methods of joining in aeronautical industry. As the use of composite materials in aeronautical structures has increased significantly, mainly because of weight concerns, riveted joints between metal and composite components became a common practice in aircraft structures.

Traditional procedures for the design of riveted joints are based in the assumption that the load carried by each fastener is equal [1]. However, it could be found in several literature related to fatigue and fracture that this assumption is not applicable when analyzing brittle materials, specially fibrous composites. When assessing the allowable load in materials that shows significant plastic strain, this assumption is suitable, once plastic strain redistributes the load in the joint. However, when dealing with materials that does not have significant plastic strains (such as fibrous composites), the redistribution of loads in the joint is not significant.

Rutman et al [2, 3] presented the multi-spring method to represent 3D fastener joints for MSC/Nastran. The most used approach is based on calculations of a single spring rate representing joint flexibility for a combination of fastener and plate properties. Rutman et al [4] modified your multi-spring method to model the fastener by shells and solid elements. Rutman et al [5] extended the fastener FEM formulation developed for metallic parts to enable its use with composite parts. In composite parts, the bearing stiffness depends on the direction of the fastener reaction. Because of this, the problem becomes non-linear and requires several iterations to solve it.

The Rutman papers [2–5] did not compare your results with experimental or analytical data. Thus, Rodrigo et al [6] tried to validate the multi-spring method through the tests performed by other authors. After this, Rodrigo et al [7] studied the methods that were currently used to analyze fasteners using finite element analysis and compared them with the Rutman method results.

The multi-spring method was employed in the joint that connects metal parts and composite parts when the load was applied. The load acting in the joint, and its distribution on the fasteners that attached hybrid parts (metal-composite plates) was obtained. The allowable load of the joint was evaluated through analytical and computational methods.

2 Allowable stress calculation

Accordingly with Niu [8], joints are the most common source of failure in airframe and other structures. This section is intended to define the theory and formulation used to evaluate the allowable stress both in metallic and composite components.

Accordingly with Ahn and Duffala [9], the design procedure of riveted joints is based upon it will fail under bearing or net-section modes. Indeed, as noted in Hart-Smith [10], all failure modes other than the aforementioned ones will fail prematurely at lower loads. Thus the designer should choose geometrical (such as pitch, thickness, fastener diameter and minimum edge distance) and constructive parameters (such as ply sequence in a laminate) to ensure that the joint will fail under bearing or net-section mode [11].

The fastener shear, the bearing failure and the net-section failure allowable loads are determined through the ultimate strength of the material metallic (Niu [8]).

The allowable stress in the laminate analyzed in this paper is dependent on its damage and ultimate failure stresses, which will be determined through bearing-bypass diagrams (Hart-Smith [12]).

These diagrams presents damage and ultimate stress curves as a function of the bearing and bypass stresses in the joint. Crews and Naik [13] have developed a bearing-bypass diagram for a T300/5208 Carbon/Epoxy laminate through a combined analytical and numerical study in which both tension and compression were tested. The lap-joint load was evaluated with the use of the Finite Elements Method. After plotting the ratio between the bearing stress (S_b) and bypass stress (S_{bp}) in the Diagram, the ultimate strength of the laminate was determined.

3 Finite element method applied to fastener modelling

The Multi-Springs Method was proposed by Alexander Rutman for modelling fasteners and has many advantages, highlighting the possibility to model a joint with no limitation in the number of components, in contrast to Single-Spring Technique which is limited to two components.

To apply this method, the Fastener-sheet translational and rotational bearing stiffness, Fastener bending stiffness and Fastener shear stiffness must be evaluated. The formulation used to calculate each parameter is presented in Rutman [3] for metallic components and Rutman [5] for composite components.

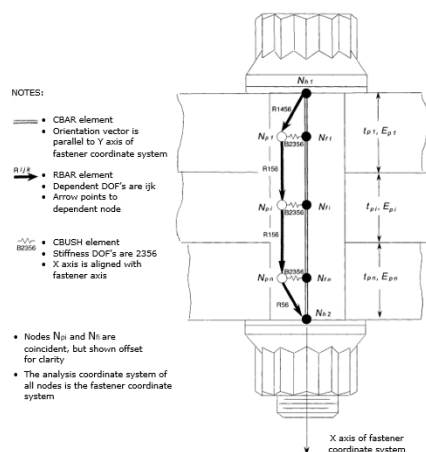


Figure 1. Elements used in Multi-Springs fastener modelling [3].

The CBAR element is used to model the fastener shank. It supports tension, compression and torsion, Moreover, supports shear and bending loads acting in X-Y and X-Z planes (see Figure 1). The CBUSH element is used to model the interface between the fastener and the components joined. It is a spring-dumper element (both linear and angular) which can link two coincident nodes in the generated mesh (nodes N_{pi} and N_{fi} in Figure 1). It has all features presented by CELASi elements, which were primarily used in the Multi-Springs method. However, CELASi element generate additional constraints in geometries that are not properly aligned [14], what deviates the model behaviour from the actual joint, issue that is overcome by CBUSH element.

The components modelled by RBAR element must be incompressible in the transverse direction (X axis in Figure 1) and the mid plane must remain parallel to each other under the load. The External faces that are in contact with fastener's head and nut must remain parallel to component's mid plane.

These conditions were stated by Rutman [3] as a way to model the rotation restraint due to the central plate in double shear connections. Indeed, without the aforementioned conditions, the plates present rotation at its edges, behaviour that does not occur in the actual joint [3].

4 Methodology

It is possible to evaluate the allowable loads of the joint, considering the load cases applied to the computational model and the methodology of assessing the loads acting on the components. It was evaluated the allowable loads for each applicable failure mode after to determine the load acting on fasteners and components and the stress acting on fasteners and components. At last, the safety margin in each component of the joint and the most critical safety margin was determined.

4.1 Joint geometry and materials

The work presented in this paper consisted in the modelling of a double shear riveted joint, which is composed by two metallic plates and a laminated plate. The joint geometry is shown by Figure 2. The lamina material and stacking sequence used in the laminate simulated in this paper are the same of Crews and Naik [13]: $[0/45/90/-45]_{2s}$, so their bearing-bypass diagrams can be used to evaluate the allowable herein determined for the composite component.

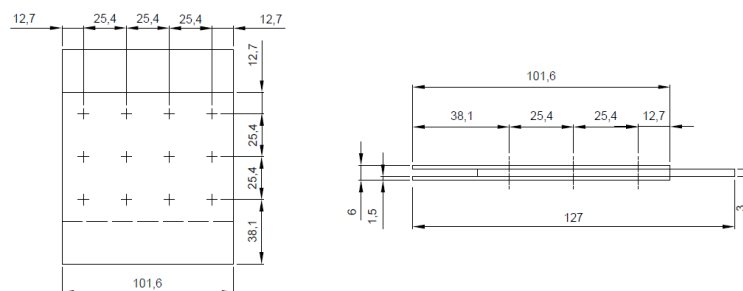


Figure 2. Joint geometry

The materials and geometrical parameters of all components used in the joint simulated are presented by Table 1.

Table 1. Material Mechanical Properties and Geometrical Parameters

| Property | 6Al-4V Annealed Titanium Alloy[15] | 2014-T6 aluminum alloy[16] | T300/5204 Graphite /Epoxy[17] |
|-----------------------------------|---------------------------------------|-------------------------------|----------------------------------|
| Young's Modulus[GPa] | 114 | 73,1 | - |
| Longitudinal Young's Modulus[GPa] | - | - | 132 |
| Transverse Young's Modulus[GPa] | - | - | 10,8 |
| Poisson's Ratio | 0,34 | 0,35 | 0,24 |
| Ultimate Shear Stress | 655 | 448 | 5,65 |
| Bearing Stress | - | 669 | - |
| Diameter [mm] | 6,35 | - | - |
| Thickness [mm] | - | 1,5 | 3,0 |

4.2 Computational model

The riveted joint presented in this work was simulated through HyperWorks software [Altair] and also has the elements needed to apply the Multi-Springs method of fastener modelling.

It was developed a computational model in order to validate the analysis developed in this work and also to evaluate the fastener behavior using the example presented Rutman [3] as a reference. The validation computational model developed is presented by Figure 3.

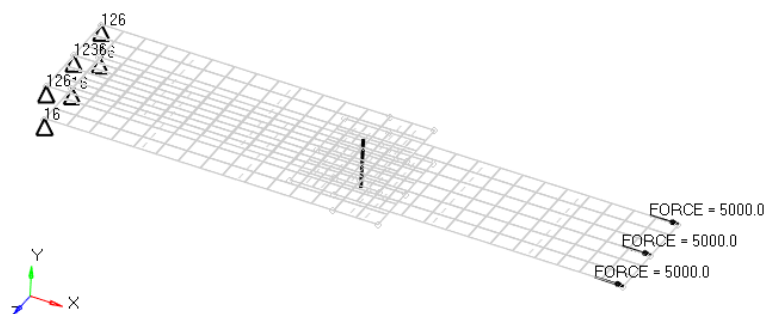


Figure 3. Validation model

The fastener deformed shape after the applying the load and boundary conditions presented in Rutman [3] is presented by Figure 4.

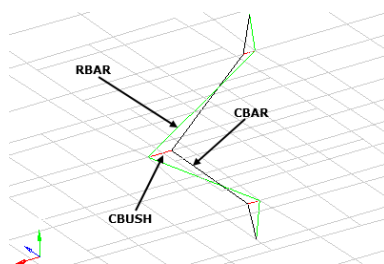


Figure 4. Fastener behavior in the validation model

After the validation of the modelling procedure, it was developed a computational model to analyse the joint presented in section 4.1. Accordingly with Rutman [5], when applying the Multi-Springs method, metallic components can be modelled both by shell and solid elements. Composite components, however, can be modelled only by shell elements. To reduce the computation time, it was used shell elements for both types of materials.

The mesh convergence was tested by comparison with the stress analysis results obtained by analytical methods. The stiffness parameters of each element applied on the fastener modelling (see figure 1) were determined using the formulation presented in Rutman [3] for metallic components and Rutman [5] for composite components and they are presented by Table 2.

4.3 Loads and boundary conditions

To determine the allowable loads of the joint, it was applied two load cases on the computational model. These loads values were arbitrarily defined as 48,0 KN in tension (negative X axis) and 48 KN in compression (positive X axis). The displacement restraints were applied on computational model through the nodes in the metallic plates. These restraints were considered as pinned, thus locking the translation in all directions.

The bearing and shear loads acting on the fasteners were determined directly through the load on CBUSH elements, once they simulate the contact between the fastener and the plates. The bypass loads around each hole were calculated from the load carried by the fasteners. The Figure 5 shows the methodology used to calculate these loads. Once the load F_a applied to component 1 is fully transferred to components 2 and 3 through the fasteners, the bypass load at point BP3 of the joint must be zero. Keeping this in mind, the bypass load at point BP2 must be equal to the bearing load acting on fastener C3. Moreover, the bypass load at point BP1 must be equal to the bearing load on fastener C2 plus the bypass load at point BP2 and so forth. Once the load acting on fasteners were already determined through CBUSH elements, this procedure is easy to apply.

Table 2. CBUSH and CBAR element stiffness parameters in fastener, fastener-metallic plate and in fastener-composite laminate interface

| Property | CBUSH | CBUSH | CBAR |
|---|----------------|-----------------|----------|
| | metallic plate | composite plate | fastener |
| Combined translational stiffness $[N/mm]$ | 71.6 | - | - |
| Combined rotational stiffness $[N.mm/rad]$ | 13.4 | - | - |
| Combined translational stiffness-x axis $[N/mm]$ | - | 104 | - |
| Combined translational stiffness-y axis $[N/mm]$ | - | 104 | - |
| Combined rotational stiffness-x axis $[N.mm/rad]$ | - | 91.4 | - |
| Combined rotational stiffness-y axis $[N.mm/rad]$ | - | 65.9 | - |
| Fastener cross-section area $[mm^2]$ | - | - | 31.7 |
| Rectangular moment of inertia $[mm^4]$ | - | - | 79.8 |
| Polar moment of inertia $[mm^4]$ | - | - | 160 |
| Factor for cross-section under shear load $[-]$ | - | - | 0.90 |

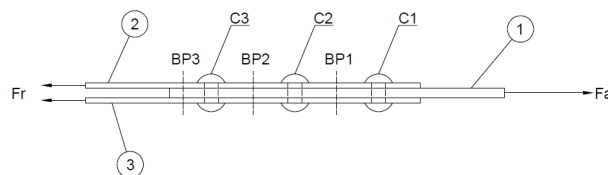


Figure 5. Joint diagram to determine the bypass load.

5 Results and discussion

The loads acting on the components of the joint, as well as its allowable loads, are presented in this section. The rivets are disposal in three rows and four columns, as shown in the Figure 2.

Through the computational model, it was possible to evaluate the load distribution in the joint, with the external fasteners being the most loaded. This behavior was expected and is in agreement with the results found in Naarayan [1]. The load distribution in the joint is shown by Table 3.

Table 3. Load distribution on the fasteners, Bypass Load distribution in the laminate and in metal sheets (%)

| Load distribution on the fasteners | | | | Load distribution in the laminate | | | Load distribution in metal sheets | | |
|------------------------------------|-----|-----|-----|-----------------------------------|-----|-----|-----------------------------------|-----|-----|
| Rows | | | | Rows | | | Rows | | |
| Column | 1 | 2 | 3 | 1 | 2 | 3 | 1 | 2 | 3 |
| 1 | 9.6 | 7.5 | 8.5 | 16 | 8.5 | 0.0 | 0.0 | 4.2 | 8 |
| 2 | 9.1 | 7.2 | 8.2 | 15.4 | 8.2 | 0.0 | 0.0 | 4.1 | 7.7 |
| 3 | 9.1 | 7.2 | 8.2 | 15.4 | 8.2 | 0.0 | 0.0 | 4.1 | 7.7 |
| 4 | 9.6 | 7.5 | 8.5 | 16 | 8.5 | 0.0 | 0.0 | 4.2 | 8 |

The bypass loads acting in both the laminate and metallic plates are presented in the Table 3 for both load cases analysed. Using the data shown in these figures, it was calculated the margin of safety for each component of the joint. The most critical values are presented in the tables 4-5 for both load cases analysed, which were found in the fasteners and holes located in edges of the first line.

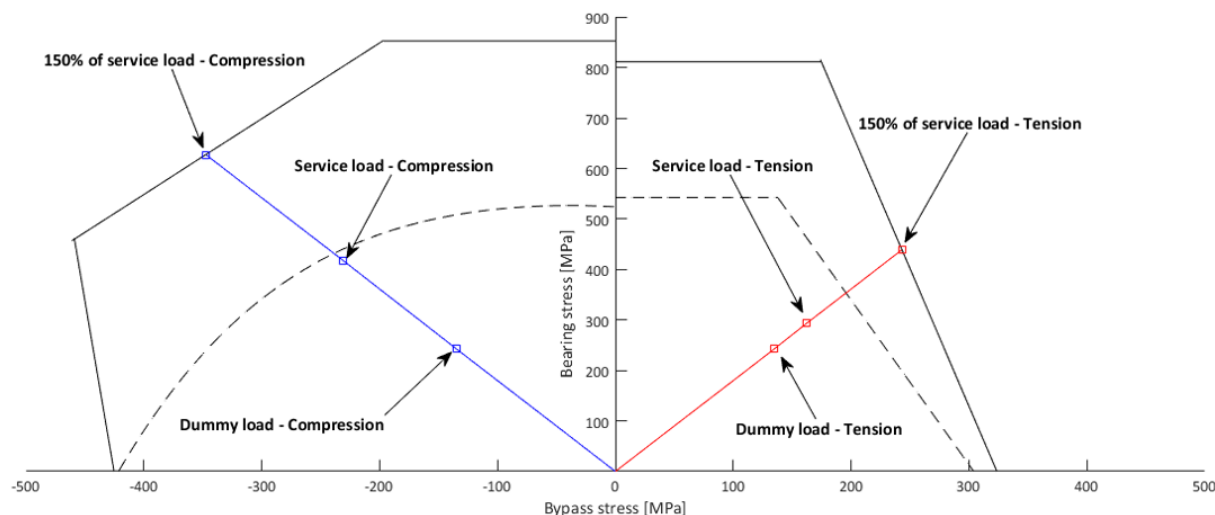


Figure 6. Bearing-Bypass diagram for the laminate simulated.

Table 4. Safety margin for the laminate - Tension and Compression load case.

| | Failure mode | Allowable stress [MPa] | Acting stress [MPa] | Margin of safety [-] |
|--------------------|--------------------|------------------------|---------------------|----------------------|
| Tension | Bearing | 293 | 243 | 0.21 |
| | Net-section | 162 | 135 | 0.21 |
| Compression | Bearing | 418 | 243 | 0.72 |
| | Net-section | -232 | -135 | 0.72 |

Table 5. Safety margin for the metallic components - Tension and compression load cases.

| Failure mode | Allowable stress [MPa] | Acting stress [MPa] | Margin of safety [-] |
|---------------------------|------------------------|---------------------|----------------------|
| Fastener shear-off | 437 | 146 | 1.99 |
| Bearing | 446 | 243 | 0.84 |
| Net-section | 298 | 144 | 1.07 |

Table 6. Joint allowable loads

| Load case | Dummy load [kN] | Margin of safety [-] | Allowable load [kN] |
|--------------------|-----------------|----------------------|---------------------|
| Tension | 48.0 | 0.21 | 58.1 |
| Compression | 48.0 | 0.72 | 82.6 |

As can be noted from the results presented above, the laminate presented the least margin of safety among the components of the joint for both load cases analysed, then governing the allowable loads, which are presented by Table6.

The allowable load under compression was 42 % greater than for the tension load case, what is in agreement with the results presented in Crews and Naik [13]. This is explained by the dual contact that occur between the fastener and the hole, what helps the joint to support more load.

Once the laminate was the most critical component in the joint and also because the load distribution affects the determination of its allowable stresses, the next figure presents the bearing-bypass diagram for the laminate simulated in this work. In this diagram was also included the bypass ratios for the most critical safety margins.

Through the previous figure, if the joint is applied in aeronautical structures, it is possible to check graphically that the allowable stresses are in agreement with PART 25[19] (dashed lines).

6 Conclusions

This paper presented the analysis of a hybrid (metal-composite) riveted joint through analytical and computational methods. Moreover, it was evaluated the load distribution in the fasteners of the joint, which were up to 16 % above the results predicted by the traditional procedure of design of riveted joints.

The evaluation of load distribution in the joint was of key importance for the analysis of the composite component, once it affects the bearing-bypass load ratios in the laminate and then the evaluation of its allowable stresses through bearing-bypass diagrams.

The allowable loads in the metallic components were not influenced by the load distribution in the joint. However, once this data is available, it is possible to improve the load distribution in the joint through the increase of stiffness in less loaded regions of the joint. It is possible to be done through the increase in plate thickness and/or the fastener diameter.

The Multi-Spring Technique made it feasible to model the double shear riveted joint presented in this paper. Moreover, it proved to be a practice and reliable way to model fasteners, even to hybrid joints, helping the designer to improve time during allowable load evaluations.

References

- [1] Naarayan, S. S., Kumar, P., & Chandra, S., 2009. Implication of unequal rivet load distribution in the failures and damage tolerant design of metal and composite civil aircraft riveted lap joints. *Engineering Failure Analysis*, vol. 16, n. 7, pp. 2255–2273.
- [2] Rutman, A. & Bales-Kogan, J., 1997. Multi-spring representation of fasteners for MSC/Nastran modelling. *Proceedings of First MSC Conference for Aerospace Users, Los Angeles, CA*.
- [3] Rutman, A., Viisoreanu, A., & Parad, J., 2000. Fasteners modeling for msc. nastran finite element analysis. In *2000 World Aviation Conference*, pp. 5585.
- [4] Rutman, A., Boshers, C., Pearce, L., & Parady, J., 2007. Fastener modeling for joining parts modeled by shell and solid elements. In *Americas Virtual Product Development Conference, Detroit, MI*.
- [5] Rutman, A., Boshers, C., Pearce, L., & Parady, J., 2009. Fastener modeling for joining composite parts. In *Americas Virtual Product Development Conference, San Diego, CA*, pp. 1–28.
- [6] Martins, R. d. S., Palma, E. S., & Lorentz, A. Influence of types of discrete modelling of fasteners in fem models.
- [7] Martins, R. d. S., dos Santos, M. T., & Palma, E. S. Influence of fastener modeling in finite elements in the load distributions in riveted joints.
- [8] Niu, M. C.-Y., 1997. *Airframe stress analysis and sizing*. Conmilit Press Hong Kong.
- [9] Ahn, J. & Duffala, N., 2010. Metal-to-metal and metal-to-composite bonded and bolted structural joints. *Encyclopedia of Aerospace Engineering*.
- [10] Hart-Smith, L., 2003. Design and analysis of bolted and riveted joints in fibrous composite structures. In *Recent advances in structural joints and repairs for composite materials*, pp. 211–254. Springer.
- [11] Handbook, M., 1997. Mil-hdbk-17-3e - composite materials handbook - volume 3: Polymer matrix composites materials usage, design, and analysis.
- [12] Hart-Smith, L., 1995. An engineer's viewpoint on design and analysis of aircraft structural joints. *Proceedings of the Institution of Mechanical Engineers, Part G: Journal of Aerospace Engineering*, vol. 209, n. 2, pp. 105–129.
- [13] Crews Jr, J. & Naik, R., may1987. Bearing-bypass loading on bolted composite joints. *NASA TM 89153*.
- [14] Nastran, N., 2014. Element library reference. *Plano, TX: Siemens PLM Software*.
- [15] Handbook, A. M., 1990. *Properties and selection: nonferrous alloys and special purpose materials*. American Society for Metals.
- [16] HANDBOOK, M., 1998. *MIL-HDBK-5H: Metallic Materials and Elements for Aerospace Vehicle Structures*. US Department of Defense. p.3-244.
- [17] Zhao, W. & Kapania, R. K., 2016. Vibration analysis of curvilinearly stiffened composite panel subjected to in-plane loads. *AIAA Journal*, vol. 55, n. 3, pp. 981–997.
- [Altair] Altair. Hyper works manual.
- [19] FAA, 2020. *FEDERAL AVIATION REGULATIONS - PART 25*.